

## IMPELLER-BLADE FAILURE ANALYSIS

### PREISKAVA POŠKODBE LOPATICE ROTORJA

Roman Celin, Franc Tehovnik, Franc Vodopivec, Borut Žužek

Institute of Metals and Technology, Lepi pot 11, 1000 Ljubljana, Slovenia  
roman.celin@imt.si

Prejem rokopisa – received: 2013-01-10; sprejem za objavo – accepted for publication: 2013-01-31

The axial pumps are used in a wide variety of applications, such as drainage control, power plants and process cooling. A fresh-water, vertical, axial-pump, stainless-steel impeller failed. The impeller was a single cast from stainless steel. A visual examination indicated that the fracture originated near the blade-to-hub attachment. During the investigation standard nondestructive and destructive methods were used. Specimens from the failed blades were taken for a material characterization. The goal of the examination was to determine a possible cause for the impeller-blade failure. After the examination it was determined that the most probable cause for the impeller-blade failure was the fatigue stress.

Keywords: blade, impeller, cast stainless steel, crack

Aksialne črpalke se uporabljajo za različne namene, kot so namakanje, hlajenje procesne opreme in komponent termoelektrarn. Lopatica rotorja vertikalno postavljene aksialne črpalke se je nepričakovano poškodovala. Lopatica in rotor sta bila ulita iz nerjavnega jekla kot celota. Vizualna preiskava rotorja je odkrila razpoko na vstopnem robu lopatice v bližini pesta. Med preiskavo vzroka nastanka poškodbe so bile uporabljene standardizirane porušitvene in neporušitvene metode. Iz lopatice rotorja so bili izdelani preizkušanci za karakterizacijo materiala. Namen preiskave je bil odkriti verjeten vzrok za poškodbo lopatice. Po končani preiskavi je bilo ugotovljeno, da je najbolj verjeten vzrok za nastanek razpoke utrujanje materiala zaradi vibracij lopatic rotorja.

Ključne besede: lopatica, rotor, lito nerjavno jeklo, razpoka

## 1 INTRODUCTION

Centrifugal pumps are turbomachines used for transporting liquids by raising a specified volume of the flow to a specified pressure level. The basic centrifugal-pump components are: the casing, the bearing housing, the pump shaft and the impeller.<sup>1</sup> A pump configuration of the components may vary depending on the fluid-flow direction that can be radial, semi-axial or axial. Axial-flow pumps achieve larger flow rates than radial pumps and are used in drainage control, power plants and process cooling. **Figure 1** shows a generic design of a vertical, axial, centrifugal pump with the main components.

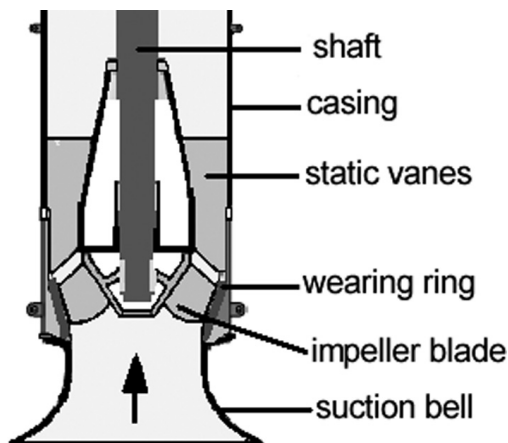


Figure 1: Vertical, axial, centrifugal pump  
Slika 1: Vertikalna aksialna centrifugalna črpalka

Any pump operation is determined by the flow rate  $Q$  ( $\text{m}^3/\text{s}$ ), the head  $H$  (m) and impeller revolutions  $n$  ( $\text{min}^{-1}$ ). The head is the measurement of the height (m) of the liquid column the pump creates from the kinetic energy that the pump gives to the liquid. The design and operation of a pump also depends on the operation efficiency, the stability of the head-capacity characteristic, vibration and noise. An important issue is also a possible pump failure due to fatigue, cavitation, hydroabrasive wear or erosion corrosion. Most vertical pumps are out of sight during the operation and, for this reason,



Figure 2: Damaged impeller blade  
Slika 2: Poškodovana lopatica rotorja

it is important to monitor the shaft vibrations and other operational parameters.

Twelve months after a plant outage a vertical, axial-flow, fresh-water pump, stainless-steel impeller failed. The hub and impeller blades were a single cast made of the ASTM A743 stainless steel (grade 316). This stainless-steel grade was a material of choice because of its good erosion-resistant properties. The axial-pump flow rate was  $Q = 8.453 \text{ m}^3/\text{s}$ , the head was  $H = 13.72 \text{ m}$  and the number of revolutions was  $n = 370 \text{ min}^{-1}$ . A complete pump assembly was dismantled and the maintenance crew immediately discovered a very distinct crack on an impeller blade (**Figure 2**). The pump owner decided to carry out a failure analysis.

A failure analysis is a broad discipline that includes materials and mechanical engineering. The purpose of this paper is to present a failure-analysis procedure applied in the case of an impeller-blade failure investigation at the Institute of Metals and Technology (IMT, Ljubljana, Slovenia).

## 2 EXAMINATION PROCESS

The failure analysis is explained in books<sup>2-6</sup> and papers.<sup>7-11</sup> The examination process starts when a component under observation has lost its designated function in a system. In general, the examination process or analysis of a damaged component is performed in several steps, which are described below. The first step is usually the on-site visit and the gathering of all the available information on the failed component and the in-service conditions of the component.

The next step includes nondestructive examinations. There is a variety of nondestructive techniques available<sup>12</sup>. The search for material imperfections is performed with X-ray, magnetic particle, ultrasonic, liquid penetrant, eddy current, and other nondestructive testing procedures. The most common is the visual examination aiming to determine the general mechanical and structural conditions of the components. The result of a visual examination is a record in the form of a sketch, dimension-measurement data or a photography, identifying discontinuities or imperfections on the surface of the components such as cracks, wear, tear, corrosion, erosion, etc.

Based on the results of a visual examination and the on-site information further decisions on the course of the examination are made. Usually that means establishing a plan for a destructive testing that involves the cutting off a sample material from the failed component, and an investigation of the samples in a laboratory for a chemical analysis, metallography, a mechanical testing and others depending on the testing plan.

A chemical analysis is performed on the original material to verify if the material sample meets the appropriate specification or standard, and whether a deviation from the specifications could have contributed to the failure. A wet chemical analysis, atomic absorp-

tion, X-ray photoelectron, Auger electron and inductively coupled plasma-mass spectrometry (ICP MS) are some of the suitable methods of a chemical analysis.

The tensile test is one of the most frequently used tests for evaluating the mechanical properties of materials.<sup>13</sup> A tensile force is applied with a machine and a gradual elongation and the final fracture of the test samples are obtained. The tensile test provides the force-extension data that can quantify the quasi-static mechanical properties of a material: yield strength, ultimate tensile strength, elongation and reduction of area at fracture.

Charpy (CVN) toughness tests are widely used to determine the impact toughness of a material and the effect of temperature on the sensitivity of structural steels to brittle fracture. Notched specimens are submitted to the impact of a hammer with the kinetic energy of 300 J. The fracturing occurs in a ductile, mixed or brittle mode and, accordingly, very different quantities of energies are consumed.

A careful investigation of the macrostructure and microstructure of a failed material can provide the most important information. A macroscopic examination of a component sample evaluates the surface of the component sample at a low magnification (usually up to 10 times). The type of a fracture such as ductile, brittle or torsion can be identified.

Metallographic examinations are performed with an appropriate magnification of optical and scanning electron microscopes (SEM). During an optical microscopic examination the grain size, microcracks, the general microstructure and inclusion content are determined. Scanning electron microscopy is used to determine small details of a microstructure, fracture, precipitate size and distribution and characteristics of crack initiation and propagation. Furthermore, with the use of an energy dispersive analysis (SEM/EDS) corrosion products on a fracture surface can be identified. It is useful to compare the microstructure of the samples removed from a failed component with the samples removed from the sound sections of a component.

A collection of visual, metallographic and SEM results along with a chemistry analysis, mechanical data and on-site information provides a solid ground for an examiner to put together conclusions on the causes and mechanism of a component failure. This is no easy task, because, in many cases, the failure reasons are not obvious even if a lot of information is available. Sufficient experience in a failure analysis is necessary to identify the cause of a failure.

## 3 RESULTS AND DISCUSSION

### 3.1 Visual examination

Only a visual examination<sup>14</sup> was performed on the failure site. The stainless-steel impeller (**Figure 3**) was a cone-shaped hub with an approximate thickness of 35 mm with six blades attached. The blades vary in thick-

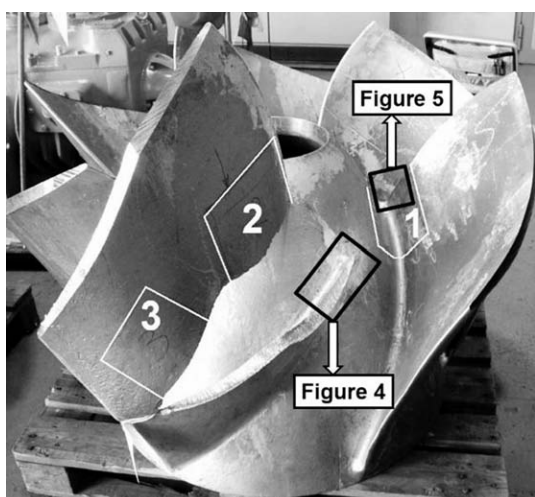


**Figure 3:** Positions of **Figures 4** and **5** with samples 1, 2 and 3 before the removal

**Slika 3:** Položaj **slika 4** in **5** ter oznake vzorcev 1, 2 in 3 pred odvzemanom

ness from approximately 25 mm near the hub to an average of 10 mm at the top of the blade. **Figures 2** and **3** show that the cast surface of the blades and the hub was not ground. Several areas were detected on the blades and at the attachment zone of the blades and the hub (**Figures 4** and **5**) where weld-repair work on the cast was performed by the supplier.



**Figure 4:** Crack surface with a repair-weld build up at the blade leading-edge attachment to the hub

**Slika 4:** Površina razpoke z reparaturnim zvarom na stiku čela lopatice in pesta

**Table 1:** Chemical-composition comparison in mass fractions (w%)

**Tabela 1:** Kemijske sestave materiala rotorja v masnih deležih (w%)

	Cr	Ni	Mo	Mn	Si	P	C	S	N
sample 1	17.5	9.73	2.05	1.07	1.03	0.022	0.03	0.003	0.044
material test report	19.2	9.6	2.3	1.08	1.28	0.03	0.01	0.01	–
ASTM A 743 CF3M	17-21	9-13	2-3	1.5	1.5	0.04	0.03	0.04	–



**Figure 5:** Crack at the leading edge of the blade

**Slika 5:** Razpoka na vodilnem robu lopatice

The top of the blade started to rub against the inner ring surface and possibly the impeller operated in a damaged condition for some time. The material loss at the top of the blade, caused by friction wearing, is noticed on **Figure 3**.

The most obvious feature on **Figures 2** and **3** is the blade splitting over the entire hub. The crack propagated at an angle of approximately 30°–35° from the blade leading edge toward the outer edge. The visual examination of the other blades revealed a through-thickness crack at the leading edge of the blade marked as sample 1 and it is shown, in detail, on **Figure 5**.

The crack initial point on both blades (**Figures 3, 4** and **5**) was above the weld-heat-affected zone. It was not possible to determine the exact initial point of the crack on the blade leading edge. The crack surface was smooth and mostly plastically deformed due to the surface grinding during the pump operation.

Three samples (**Figure 3**) were chosen for further analysis. **Figure 5** shows sample 1 which was used for a fracture analysis, while samples 2 and 3 were used for manufacturing the tensile and Charpy V-notch specimens.

### 3.2 Chemical analysis

A quantitative chemical analysis was performed on the impeller-blade sample material. It was made with an ICP mass spectrometer. The results of the composition analysis are shown in **Table 1**.

The sample-1 chemical-composition-analysis results and impeller-manufacturer material-test report were in accordance with the ASTM grade A743 (316L) cast stainless-steel specification requirements presented in **Table 1**.

### 3.3 Mechanical testing

A series of standard tensile tests<sup>15</sup> and impact tests<sup>16</sup> were performed with the specimens machined from the samples shown in **Figure 1**. The goal of the standard mechanical tests was to find out if the sample material was in accordance with the manufacturer’s material-test report and the ASTM specification. The tensile-test results are presented in **Table 2**.

**Table 2:** Tensile-test results

**Tabela 2:** Rezultati nateznega preizkusa

	Yield strength $R_{p0.2}$ /MPa	Tensile strength $R_m$ /MPa	Elongation $A$ /%
sample 2			
1	262	524	57
2	284	527	59
3	301	562	64
material test report			
US units	48 PSI	91 PSI	30
ASTM A 743 specification			
SI units	min. 205	min. 485	30
US units	min. 30 PSI	min. 70 PSI	30

The yield-strength and tensile-strength results for the three machined specimens are in accordance with the manufacturer’s material-test results and ASTM specification requirements.

The Charpy impact tests were performed at room temperature, according to the SIST EN standard, on a testing machine with an impact pendulum of a 300 J capacity. The Charpy-test results on the three V-notch samples were 250 J, 203 J and 261 J of the absorbed pendulum energy, which is above the minimum required value of 100 J from the owner’s specification.

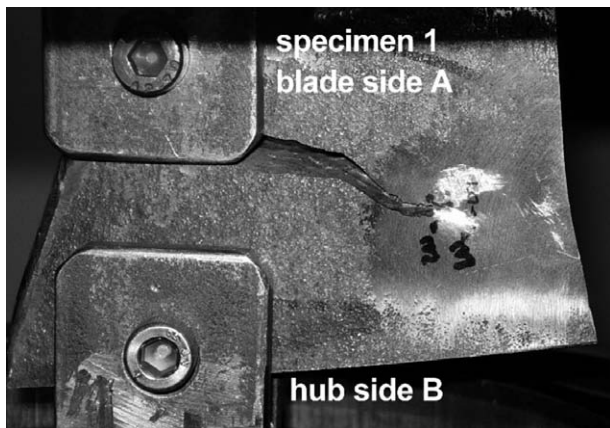


**Figure 6:** Sample-1 crack opening on a tensile-testing machine  
**Slika 6:** Razpiranje vzorca 1 na trgalnem stroju

**Figure 6** shows sample 1, cut from the hub, clamped on the tensile-testing machine with the purpose to obtain the fracture surface without any grinding or other damage.

### 3.4 Metallographic examination

**Figure 7** shows the cast A743-steel microstructure of the hub at the blade side B of specimen 1 and **Figure 8** shows the microstructure of the blade leading edge (side A).

It consists of dendritic austenite grains with the inserts of  $\delta$  ferrite at some grain boundaries. The content of the  $\delta$  ferrite was of about 5 %. The microstructure shown on both pictures is without any peculiarity and it is typical for the cast stainless steel.

### 3.5 Scanning electron microscopy (SEM)

**Figure 9** shows the side-A fracture-surface view. The bright area (marked as 1.2) on the right is the fracture

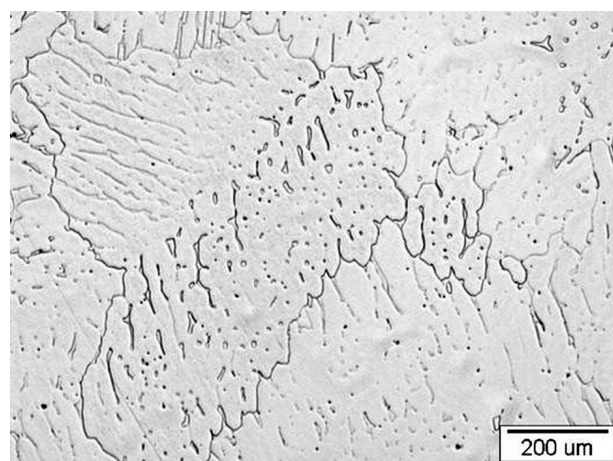


**Figure 7:** As-cast microstructure of the hub-to-blade attachment  
**Slika 7:** Mikrostruktura ulitka na stiku pesta in lopatice

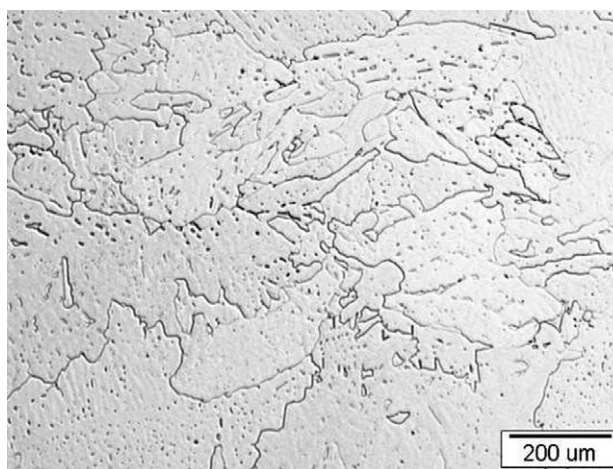


**Figure 8:** Microstructure of the blade leading edge (sample 1 – side A)  
**Slika 8:** Mikrostruktura roba lopatice (vzorec 1 – stran A)

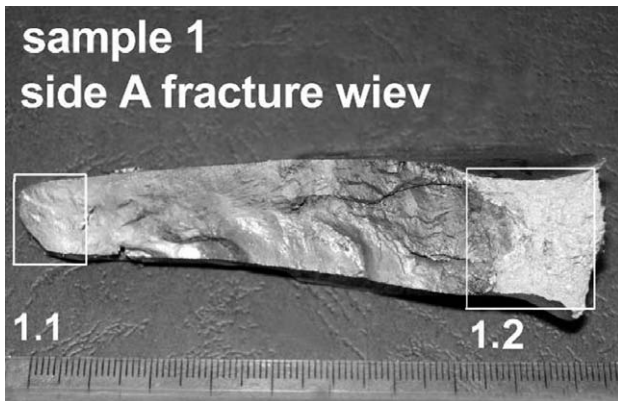


**Figure 9:** Side-A fracture surface of sample 1  
**Slika 9:** Površina preloma na strani A vzorca 1



**Figure 10:** SEM image of plastically deformed surface area 1.1  
**Slika 10:** SEM-posnetek deformirane površine, označene z 1.1

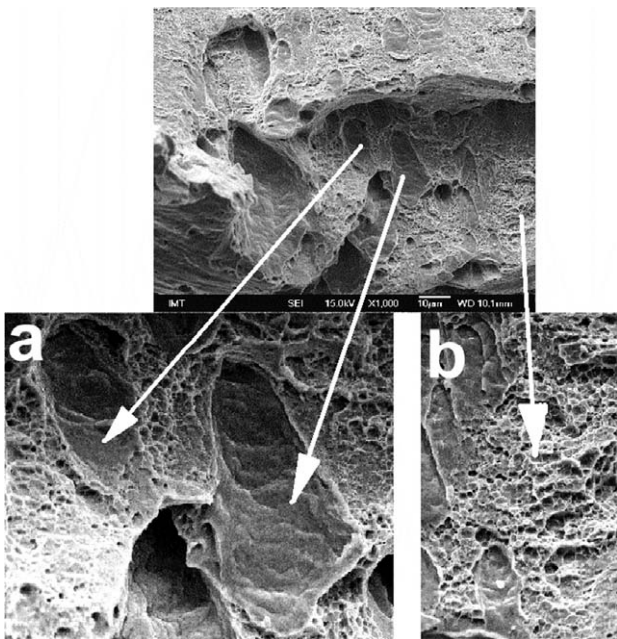


**Figure 11:** a) Interphase fracture and b) ductile fracture  
**Slika 11:** a) Medfazni in b) žilav prelom

surface obtained by tensile-machine crack opening (**Figure 6**).

The sample-1 side-A fracture surface has the same features as the fracture surface shown on **Figure 4**. The surface is smooth and the mostly plastically deformed area marked as 1.1 (**Figure 9**) was carefully examined with an optical microscope. Because of the plastically deformed surface, the exact crack point of origin was impossible to ascertain. Also, the crack propagation mode could not be distinguished on the damaged surface (**Figure 10**) and the fatigue striations were not detected either.

The area (marked as 1.2 on **Figure 6**) enabled a SEM investigation of the fracture surface, and **Figure 11** shows two fracture modes. One (**Figure 11 a**) presents an interphase crack propagation on the interface of austenite and the inserts of  $\delta$  ferrite, while the other (**Figure 11 b**) looks like a ductile fracture with small dimples.

#### 4 CONCLUSIONS

The examination procedure described was performed to determine the mechanism of a failure of stainless-steel impeller blades. According to the owner's data the impeller operated within the design parameters. For the given application, the impellers appear to have been fabricated within the tolerances and specifications required by the owner. The surface of the hub and blades was as cast. In general, an as-cast condition of a surface as well as the weld-repair places are sensitive regions prone to a crack formation because of dynamic loading.

The metallographic examination did not reveal a deteriorative influence of a weld on the microstructure around the crack-initiation area. The crack-initiation point could not be determined because of the deformed surface.

After the examination it was concluded that the most probable cause for the impeller-blade failure was the fatigue caused by the flow-induced vibrations due to a turbulent flow over the blades and the internal stresses caused by the welding repair of the casting defects.

The crack-initiation point on the blade leading edge was probably a weak spot between the columnar dendritic grains of the cast.

#### 5 REFERENCES

- 1 J. F. Gülch, Centrifugal pumps, Springer-Verlag, Berlin 2008, 61 or 368
- 2 K. A. Esakul, Handbook of case histories in failure analysis, Vol. 1, ASM International, 1992, 251
- 3 H. M. Tawancy, A. Ul-Hamid, N. M. Abbas, Practical engineering failure analysis, Marcel Dekker, New York 2004, 14
- 4 W. T. Becker, R. J. Shipley, ASM Handbook, Vol. 11, Failure analysis and prevention, Materials Park: ASM International, 2002, 316
- 5 A. K. Das, Metallurgy of failure analysis, Mc Graw-Hill, New York 1997, 55

- <sup>6</sup> C. Brooks, A. Choudhury, Failure analysis of engineering materials, Mc Graw-Hill, New York 2002, 8
- <sup>7</sup> M. Torkar, F. Tehovnik, M. Godec, Mater. Tehnol., 46 (2012) 4, 423–427
- <sup>8</sup> A. van Bennekom, F. Berndt, M. N. Rassol, Eng. Failure Analysis, 8 (2001) 2, 145–156
- <sup>9</sup> M. Muhič, J. Tušek, F. Kosel, D. Klobčar, M. Pleterški, Thermal fatigue cracking of die-casting dies, Metallurgy, 49 (2010) 1, 9–12
- <sup>10</sup> G. Kosec, A. Nagode, I. Budak, A. Antić, B. Kosec, Failure of the pinion from the drive of a cement mill, Eng. Failure Analysis, 18 (2011) 1, 450–454
- <sup>11</sup> R. B. Setterlund, V. K. Malhotra, L. K. Friesen, Failure of 13 % Chromium Stainless Steel Impeller From Hydrogen Recycle Compressor, Proc. of the Corrosion 2000, Orlando, USA, 2000
- <sup>12</sup> ASM Handbook, Volume 17, Nondestructive Evaluation and Quality Control
- <sup>13</sup> ASM Handbook, Volume 8, Mechanical Testing and Evaluation
- <sup>14</sup> SIST EN 13018, Non-destructive testing – Visual testing – General principles
- <sup>15</sup> SIST EN ISO 6892-1, Tensile testing, Method of test at ambient temperature
- <sup>16</sup> ISO 148-1, Charpy pendulum impact test